High Frequency Phase Variable Model of Electric Machines from Electromagnetic Field Computation

O. A. Mohammed, S. Ganu, N. Abed, S. Liu, and Z. Liu

Department of Electrical and Computer Engineering
Energy Systems Laboratory
Florida International University, Miami, FL 33174, USA

Abstract — This paper presents a high frequency phase variable model of electric machines obtained using finite element (FE) analysis. The model consists of the low frequency phase variable model in parallel with a high frequency winding branch. The resistance and inductance of individual winding turns are calculated by magnetodynamic FE analysis while capacitance is calculated by electrostatic FE analysis. With the obtained parameters, a distributed model was formed based on the winding arrangement. The order of the distributed winding model is reduced using the Kron reduction technique to form the lumped parameter high frequency winding branch. A Permanent Magnet synchronous motor (PMSM) with its operating inverter is used as an example. The developed model is then used to evaluate the motor-inverter interaction. The results show the ability of the developed model to represent the motor's high frequency behavior under different operating conditions.

Index Terms — FE, high frequency, PM synchronous motor, Kron reduction, phase variable model, lumped parameters, distributed parameters

I. INTRODUCTION

Many efforts have been devoted to develop the high frequency induction motor models based on experiments. Using these models, the overvoltage at the machine terminals, electromagnetic interference, and voltage distribution among the winding turns have been reported [1, 2]. A conventional direct–quadrature (dq) axis model of PMSM has also been developed using an experimental approach [3]. The model can represent the motor's low and high frequency behaviors.

In this paper, an FE based physical motor model of randomly wound PMSM is developed. The developed model can be used to test, improve, and optimize the motor design. This model consists of a high frequency branch connected in parallel with a low frequency phase variable model. The low frequency phase variable model represents the motor's low frequency behavior while the high frequency winding branch represents the high frequency behavior. A change in the winding arrangement will affect only the high frequency winding branch parameters and will not affect the low frequency phase variable model parameters.

The FE based approach is used to calculate the high frequency model parameters. The developed model is used to evaluate the integrated motor drive high frequency behavior. This includes the motor terminal overvoltage, effect of switching frequencies on the motor currents and output torque. The simulation results show the ability of the developed model to represent the motor low and high frequency behavior under various dynamic operating conditions.

II. HIGH FREQUENCY WINDING BRANCH PARAMETER CALCULATION USING FE

A 2-hp, 6-poles, 36-slots, random wound winding arrangement, with 128 amp-turns per half slot motor was used as an example. Due to the symmetry, a one pole of the motor's geometry is used considering the individual turns in each half slot as shown in Fig. 1. Each slot contains 18 turns with 9 turns in each half slot. Each turn utilizes #14 gauge wire with diameter of 1.6281 mm. Diameter of insulation is 1.73 mm. The same positioning of the turns within the other slots is maintained. To consider the geometry effects on the inductance and capacitance, all the slots in one pole of the motor's geometry were modeled. The winding resistance, inductance and capacitance values are function of the operating frequency. The resistance increases with the increase in the supply frequency due to the skin and proximity effects. The skin effect is the tendency of the current to remain at the surface region of the conductor while the proximity effect is the action of the magnetic field of adjacent conductors on the current density distribution inside the given

conductor. The inductance value decreases with the increase of the frequency. The change in the capacitance values with the change in the frequency is minimal and can be ignored in the considered frequency range. The capacitances are distributed between turn to turn and turn to ground. The capacitance provides an easy path for high frequency current components to flow between the turns and to ground.

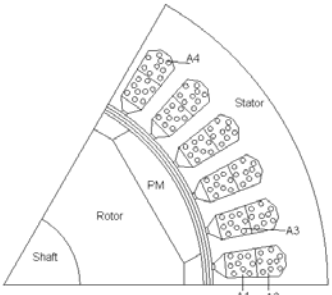

Fig. 1. One pole motor geometry with individual winding turns.

A 2-D magnetodynamic FE analysis is performed to obtain resistances and inductances of the different winding turns. This analysis is a steady state time harmonic form of diffusion equation [4]. First a geometry description is set up by assigning the proper material properties to the different parts of the one pole geometry. The rotor and stator iron are composed of nonlinear magnetic material with linear resistivity. The turn conductors are assigned with unit permeability and resistivity. Assignment of resistivity is required to include the eddy current effects. The motor magnets are assumed to be linear. The shaft, fixing wedge and insulation inside the slots were assigned with air. The meshing is selected in coordination with the skin depth. The size of the mesh elements inside each turn is kept less than the skin depth. The skin depth is calculated according to the rise time of the pulse width modulation (PWM) pulses. The rise time of the PWM pulse is $1\,\mu$s which corresponds to the frequency component of 1-MHz. The skin depth at 1-MHz frequency is 6.6 e-5 m. The meshing details inside the one pole model are shown in Fig. 2. The mesh contains 7937 line elements and 179692 surface elements.

Periodic boundary conditions are assigned to the wedge shaped pole structure while the homogeneous Dirichlet boundary conditions are applied to the outer stator surface. The FE-circuit coupling allows us to simulate the exact operating conditions with real voltage supply connection. The field and circuit equations are coupled and solved simultaneously [5]. The magnetic field inside the motor is governed by the following partial differential equation

$$\nabla \times H = J_s + J_e \tag{1}$$

where, J_s is the source current density, J_e is the induced current density, and H is the field intensity. In general, the current in the circuit domain with m loops can by represented by the following set of equations

$$[E_m] = [R_m][I_m] + [L_m]\frac{\mathrm{d}}{\mathrm{dt}}[I_m] + \left[\frac{1}{C_m}\right]\int I_m dt + [\gamma_m] \tag{2}$$

where, R_m represents the matrix of resistances, L_m is the matrix of inductances, C_m is the matrix of capacitances, γ_m is the matrix of non-linear voltage drops, I_m is the matrix of currents, and E_m is the matrix of voltages. More details about the formulation can be found in [5].

The inductance and resistance frequency response of the different turns were obtained by solving the magnetodynamic problem for various supply frequencies. The frequency range used is from 10-kHz to 1-MHz. Usually the PWM switching frequencies are in the range of tens of kHz. The upper limit of the frequency range is selected to include harmonics up to 1-MHz.

The computation took 4 hours to solve the magnetodynamic problem on a Pentium P4, 3-GHz machine. During the simulation all the turns were connected in series. After solving the coupled field circuit problem, the resistances and inductances as functions of frequency were obtained.

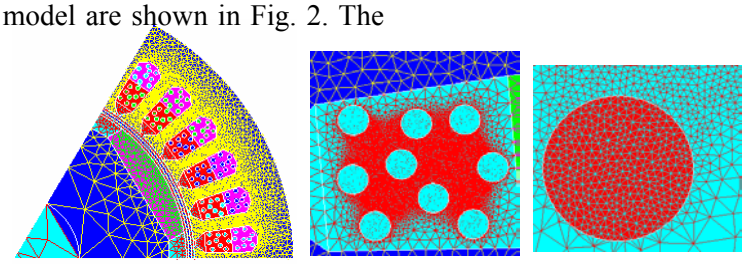

Fig. 2. Mesh details inside one pole model, inside slot and inside turn.

The variation of the resistance and the inductance versus the frequency for different turns in the first half slot of phase A are shown in Figs. 3 and 4, respectively.

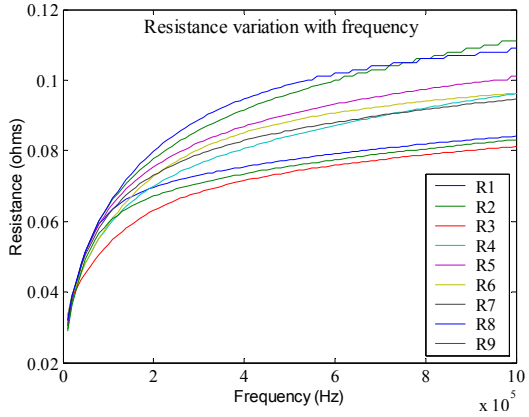

Fig. 3. Resistance variation with frequency.

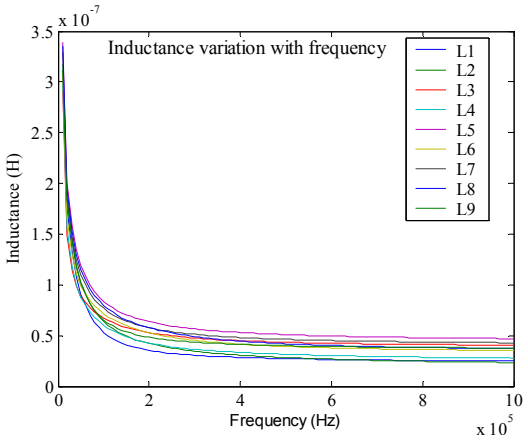

Fig. 4. Inductance variation with frequency.

In Figs. 3 and 4, R_1, R_2… and L_1, L_2… correspond to the resistance and the inductance of the different turns in the first half slot of phase A respectively. It is difficult to point out each individual turn in Figs. 3 and 4, since all the curves are very close to each other. Therefore, the figures are just meant to show the trend of variation of resistance and inductance with frequency. It should be noted that the slope of the resistance curve becomes smaller and also the slope of inductance curve becomes constant in the higher frequency region. The inductance obtained by this method is apparent global inductance. Since simultaneous excitation of all the turns in a given half slot is performed, the inductance value contains both self and mutual inductance terms. The skin effect inside the iron is more pronounced compared to the turn conductors. As a result, the flux lines do not penetrate the iron region but remain confined inside the slot. Figure 5(a) shows flux plot at 30 kHz frequency while Fig. 5(b) shows the flux plot at 1-MHz frequency. The flux plots are at steady state. These figures clearly show the fact that the stator iron acts as a flux barrier due to the increased eddy currents at high frequency. The position and numbering of turns in the first slot is also shown in Fig. 5(b). Similar calculations were repeated for each half slot.

The capacitances were calculated from FE electrostatic analysis since capacitances are function of the motor geometry and not the supply frequency. The electric field is assumed to be linear in this case and it is proportional to the applied voltage. The analysis determines the electric scalar potential distribution due to the applied voltage [6]. The turn conductors were treated as perfect conductors and hence are not meshed. The insulation in the slot and surrounding of the conductor is finely meshed. The mesh details in the slot and the insulation is shown in Fig. 6(a-c). The capacitance calculation is based on the energy principle. By applying voltage on the conductors, the ground capacitance matrix was calculated from the stored static energy. The electric potential distribution inside the motor is governed by the following partial differential equation,

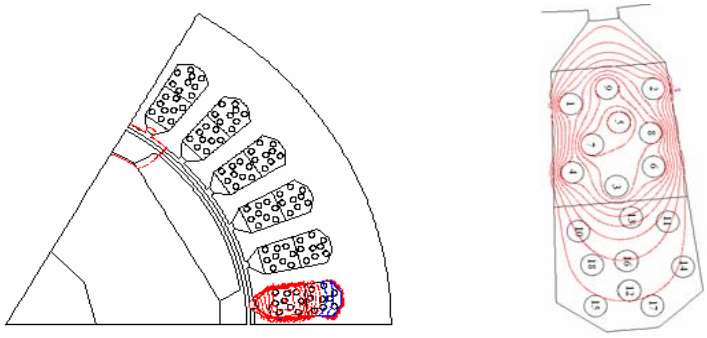

(a) (b)

Fig. 5.(a) Flux lines in one pole machine at 30 kHz, (b) In the slot at 1 MHz.

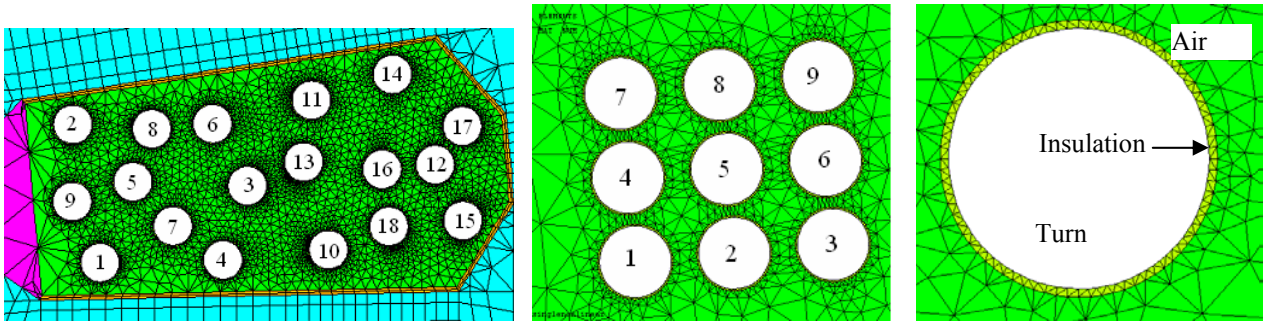

(a) (b) (c)

Fig. 6. Mesh details (a) inside one slot, (b) inside half slot, and (c) surrounding single turn.

$$\nabla\bullet\left(\varepsilon_r\varepsilon_0\nabla V\right)=-\rho \tag{3}$$

where, ρ is surface charge density, ε_r is relative permittivity, ε_0 is air permittivity, and V is electric scalar potential.

To calculate the lumped capacitance matrix, charges are related to the potential differences. Similar capacitance calculations were repeated for each half slot. The mutual capacitances were calculated between turns within each half slot. All capacitances were multiplied by the mean length of the turn as the calculated capacitances are per unit length. The self capacitance is the addition of the ground capacitance and mutual capacitances with other turns.

III. DISTRIBUTED PARAMETER MODEL AND ITS REDUCTION

The distributed parameter winding model is shown in Fig. 7. The model is formed using the high frequency parameters obtained from the FE analysis. The distributed model consists of the resistance of each turn, the global inductance of each turn, the capacitance to ground for each turn and the mutual capacitances with other turns inside the half slot. The used motor has 216 turns per phase. All the turns in a given phase are connected in series thus forming 217 nodes. The parameters of the first turn are between nodes 1 and 2; the parameters of the second turn are between nodes 2 and 3 and so on. The ground capacitance is equally distributed between the two ends of the turn. Here, C_{12} is the mutual capacitance between turns 1 and 2; R_1 and L_1 are the resistance and global inductance of the first turn, respectively. Also, C_{1g} is the capacitance to the ground of the first turn and so on. The resistance and inductance values used in the model are the average values over the considered frequency range.

The order of the distributed parameter winding model obtained above is reduced by using Kron reduction technique [7]. This reduction is performed in order to reduce the simulation time so that a global solution of the combined low and high frequency phenomena of PWM motor-inverter interaction can be obtained at much faster speeds. PWM is the modulation technique to obtain inverter output voltage control. The nodal method is used to form the admittance matrix of the distributed winding model. In this algorithm, all the nodes other than the terminal nodes are eliminated. To eliminate the internal nodes, the admittance matrix is partitioned such that the nodes to be removed are represented in the upper rows. The partitioned matrices are shown below in (4). In equation (4), i and j are terminal nodes and n is the number of turns**.** The reduced admittance matrix is obtained from (4) using matrix transformation formula given in (5),

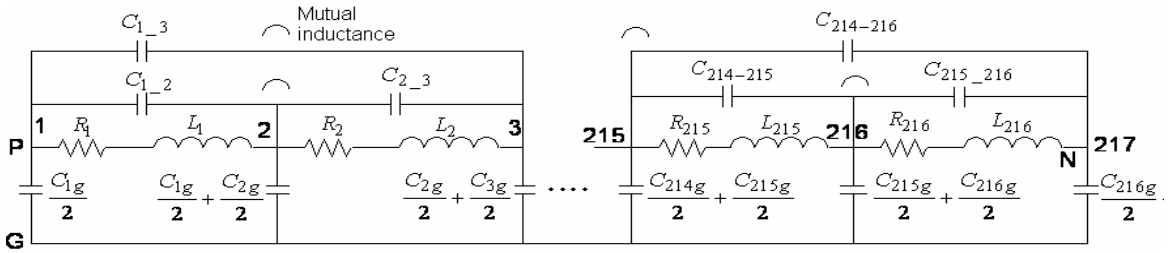

Fig. 7. Distributed parameter winding circuit obtained from FE analysis.

$$\begin{bmatrix} \begin{bmatrix} Y_{11} & \cdots & Y_{1,(n-1)} \\ \vdots & \cdots & \vdots \\ Y_{(n-1),1} & \cdots & Y_{(n-1)(n-1)} \end{bmatrix} & \begin{bmatrix} Y_{1i} & Y_{1j} \\ \vdots & \vdots \\ Y_{(n-1),i} & Y_{(n-1),j} \end{bmatrix} \\ \begin{bmatrix} Y_{i1} & \cdots & Y_{i,(n-1)} \\ Y_{j1} & \cdots & Y_{j(n-1)} \end{bmatrix} & \begin{bmatrix} Y_{ii} & 0 \\ 0 & Y_{jj} \end{bmatrix} \end{bmatrix} \quad \begin{matrix} \text{B1} \\ \\ \text{B2} \end{matrix} \quad \begin{matrix} \text{B3} \\ \\ \text{B4} \end{matrix} \tag{4}$$

$$Y_{node}^{red} = B_4 - B_3 B_1^{-1} B_2 = \begin{bmatrix} y_{11} & y_{12} \\ y_{21} & y_{22} \end{bmatrix}. \tag{5}$$

In (5), Y_{node}^{red} is the reduced (2×2) admittance matrix. The π-network model shown in Fig. 8 (a), is used to represent the resultant matrix (5) using the principle of two port circuit [8]. The obtained π-network is symmetrical with equal diagonal elements. From the π-network model parameters, the high frequency branch parameters R, L, and C_g are obtained. The lumped equivalent circuit for the high frequency branch is shown in Fig. 8 (b).

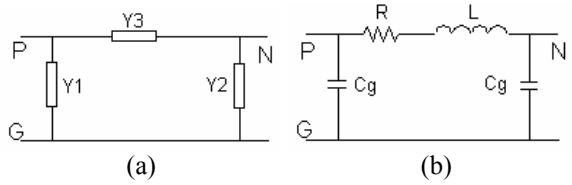

(a) (b)

Fig. 8. (a) π-network model, (b) Reduced order high frequency winding branch.

The high frequency phase variable model is shown in Fig. 9. This model consists of the low frequency phase variable model in parallel with the high frequency winding branch. The low frequency phase variable model was previously developed by the authors [9]. A filter is connected in series with the high frequency winding branch to filter out the fundamental (60 Hz) frequency components [10]. The lumped parameter values at various switching frequencies are given in Table 1. It should be observed that there is slight change in the values of the parameters by changing the winding arrangement from a form wound winding type to random wound winding type for same number of turns. Further details on the parameters of form wound winding type motor can be found in [11].

IV. SIMULATION AND RESULTS

The high frequency phase variable motor model is tested in an integrated motor drive system as shown in Fig.10. A vector control algorithm is used to drive the motor. The motor drive system consists of a PWM inverter, cable and the developed motor block model. The load torque is set to its rated value of 12 N.m.

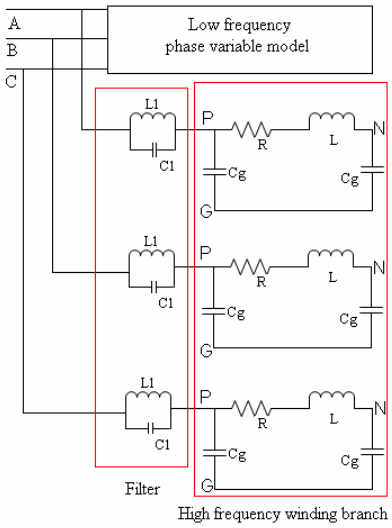

Fig. 9. High frequency phase variable model.

Table 1. Lumped parameters at different frequencies.

Per phase	10 kHz	20 kHz	30 kHz
Resistance R (Ω)	6.66	8.08	9.02
Inductance L (μH)	67.37	38.46	29.97
Capacitance Cg (nF)	1.42	1.42	1.42

As shown in Fig. 10, there are two cascaded control loops to control the motor. The inner loop controls the motor's stator currents. The outer loop controls the motor's speed. A high frequency cable model was used to connect motor to the inverter [12]. The simulation was performed at various switching frequencies namely, 10-kHz, 20-kHz, and 30-kHz. For PWM switching operation, the simulation time step should be in the range of nanoseconds in order to capture the spikes in the various waveforms. Figure 11 shows the three phase current profiles at different switching frequencies. The pulsations in the current waveform are due to PWM switching action. The spikes in the current waveform are due to high voltage edge rates of converter elements and cable parameters. The high frequency branch enables us to include these spikes. These spikes are clearly visible in 10-kHz current waveform results. At 20-kHz and 30-kHz frequency, there is an increase in

the number of current spikes since the spikes are formed at each transition point. Since the capacitance values are constant for all cases, the increase in the magnitude of current spikes is marginal. The spikes in phase A current are clearly shown in Fig. 12. Typical torque waveform is shown in Fig. 13 at various switching frequencies. The pulsations in the torque are due to the PWM switching action. The frequencies in the simulations are approximate values since the motor is working under the hysteresis current controller. Therefore the captions of Fig. 11 to Fig. 14 are annotated with (approx.) label. The spikes are also visible in the ground current which is shown in Fig. 14. This current is the current passing to the ground through high frequency winding branch. This current produces electromagnetic interference with other electrical equipments connected to the ground. The motor model is also tested for the overvoltage phenomenon when connected through a long cable to the PWM inverter. Due to the impedance mismatch between the cable impedance and the motor input impedance, the voltage builds up at motor's terminal and can reach a peak value of double the DC supply voltage. This can damage the motor's insulation. Predicting this overvoltage magnitude is very crucial in the insulation design and selection process. To investigate the effect of cable length on the motor overvoltage, the motor model is connected to a cable of different lengths. The overvoltage at 10-kHz switching frequency is shown in Fig. 15. As the length of the cable increases, the amplitude of the voltage increases and the frequency of oscillations decrease. The simulation results show that the developed model can predict motor-inverter interaction at faster speeds than full FE model. The developed model can be used to evaluate EMI issues during the design and development process numerically.

V. Conclusion

A high frequency phase variable electric machines model is developed using FE analysis. This was done numerically rather than experiments. This approach will allow us to evaluate the motor high frequency behavior during the design process. The winding arrangement changes show a little difference in the parameter values for equal number of turns. The model can predict motor high frequency behavior such as motor current spikes, terminal overvoltage as well as the ground currents at fast computation speed. The model can be utilized in design optimization and insulation selection for motors during design process as well as in the evaluation of EMI issues.

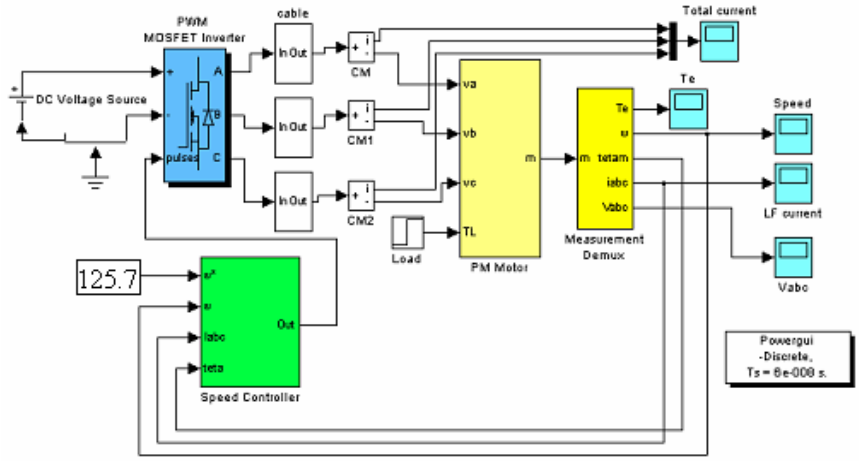

Fig. 10. Integrated motor drive system.

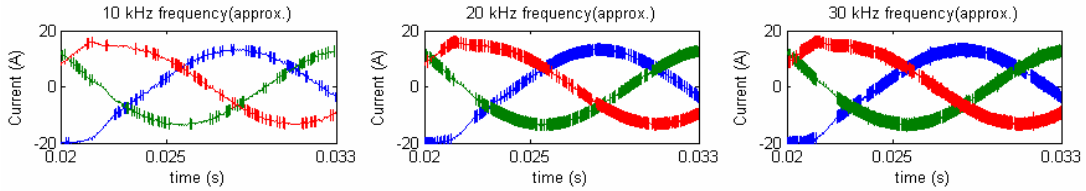

Fig. 11. Three phase steady state current waveform at different switching frequencies.

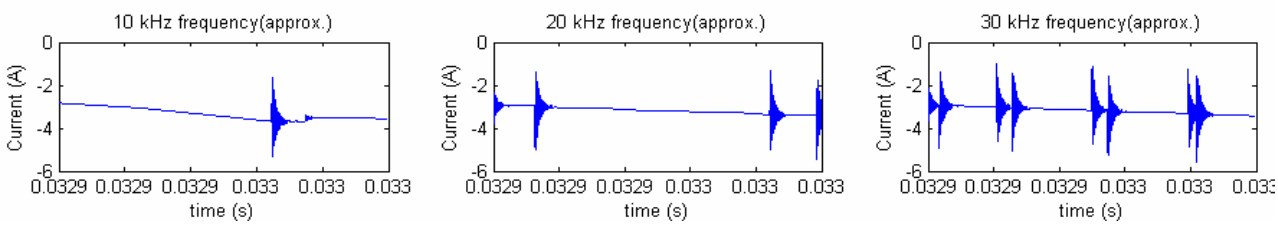

Fig. 12. Phase A steady state current waveform at different switching frequencies.

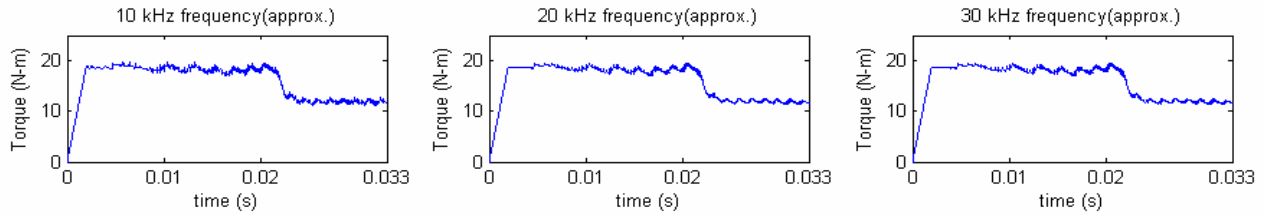

Fig. 13. Torque profile at different switching frequencies.

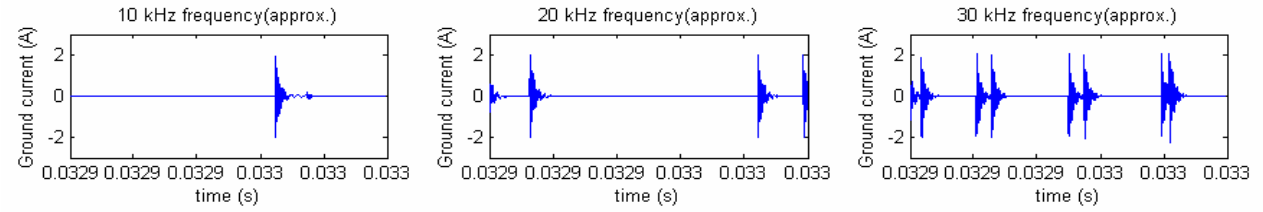

Fig. 14. Grounding current at different switching frequencies.

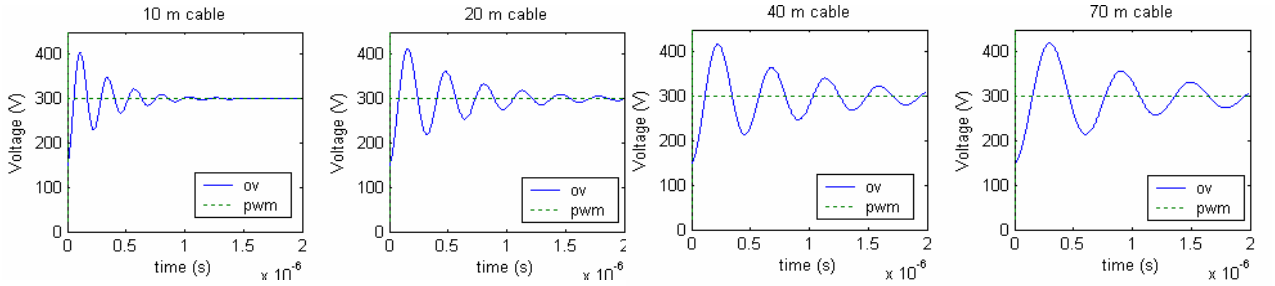

Fig. 15. Overvoltage profile for different cable lengths.

REFERENCES

[1] A. Boglietti, E. Carpaneto, "Induction Motor High Frequency Model" conf. Rec. IEEE IAS annual meeting, pp.1551-1558, 1999.

[2] H. A. Toliyat, G. Suresh, and A. Abur, "Estimation Of Voltage Distribution On The Inverter Fed Random Wound Induction Motor Windings Supplied Through Feeder Cable," IEEE Transactions on EC, Vol. 14, No. 4, pp. 976-981, Dec. 1999.

[3] S. D. Sudhoff, J. Tichenor, J. Drewniak, "Wide Bandwidth Multi-Resolutional Analysis of A Surface Mounted PMSM," IEEE Transactions on EC, Vol. 14, No. 4, pp. 976-981, Dec. 1999.

[4] S. J. Salon, "Finite Element Analysis of Electrical Machines, Kluwer academic publishers, 1995.

[5] F. Piriou and A. Razek, "Finite Element Analysis in Electromagnetic Systems Accounting for Electric Circuits," IEEE Transactions on Magnetics, Vol. 29, No. 2, pp. 1669-1675, March 1993.

[6] A. Hieke, Siemens and IBM, "ANSYS APDL for Capacitance", Proceedings from `Second International Conference on Modeling and Simulation of Microsystems, Semiconductors, Sensors and Actuators' San Juan, Puerto Rico, pp. 172, (1999).

[7] G .Kron, "Tensor Analysis of Networks," John Willey and Sons, 1939.

[8] Leonard Bobrow, "Elementary Linear Circuit Analysis," pp. 575-577.

[9] O. A. Mohammed, S. Liu and Z. Liu, "Physical Modeling Of PM Synchronous Motors For Integrated Coupling With Machine Drives," IEEE Transactions on Magnetics, Vol. 41, No. 5, pp. 1628-1631, May 2005.

[10] L. Ran, S. Gokani, J. Clare, K. J. Bradley, and C. Christopoulos, "Conducted Electromagnetic Emissions in Induction Motor Drive Systems Part I- Time Domain Analysis And Identification Of Dominant Modes," IEEE Transaction on Power Electronics, Vol. 13, No. 4, pp. 757-767, July 1998.

[11] O. A. Mohammed, S. Ganu, N. Abed, S. Liu and Z. Liu, "High Frequency PM Synchronous Motor Model Determined By FE Analysis," IEEE Transactions on Magnetics, pp. 1291-1294, April 2006.

[12] A. Moreira, T. A. Lipo, G. Venkataramanan, S. Bernet, "High Frequency Modeling For Cable And Induction Motor Overvoltage Studies In Long Cable Drives," IAS Transactions, Vol. 38, No. 5, pp. 1297-1306, Sept. 2002.

Osama A. MOHAMMED. Dr. Mohammed received his M.S. and Ph.D. degrees in Electrical Engineering from Virginia Polytechnic Institute and State University. He has many years of teaching, curriculum development, research and industrial consulting experience. He authored and co-authored more than 300 technical papers in the archival literature as well as in National and International Conference records in addition to additional numerous technical and project reports and monographs. He specializes in Electrical Power Systems, design optimization of electromagnetic devices, Artificial Intelligence Applications to Energy Systems as well as Electromagnetic Field Computations in Nonlinear Systems. He has current interest in Shipboard power systems and integrated motor drive systems. Dr. Mohammed is a fellow of IEEE and is the current president of ACES. He is editor of IEEE Transactions on Magnetics and COMPEL Journal.

Shreerang GANU. Mr. Ganu received his Bachelor degree in Electrical Engineering from Pune University, India in 1998, M.S. degree in Electrical Engineering from Florida International University Miami, USA in 2002. Currently he is working towards his Ph.D. degree in Electrical Engineering at Florida International University. His research includes computational electromagnetics applied to electrical machines, motor drives and power systems.

Nagy ABED. Mr. Abed is a Student Member of IEEE since 1997. He received the B.S. and M.S. degrees in electrical engineering from Mansoura University, Egypt, in 1996 and 1999, respectively. He is currently a Graduate Student in the Ph.D. program at Florida International University. His current academic and research interests include power systems, Finite element, Power electronics, power quality, and computer aided design of electromagnetic devices in low and high frequencies.

Dr. Shuo LIU. Dr. Liu received her Ph.D. from Hebei University of Technology, Tianjin, China in 2001. In 2001, she joined Energy Systems Laboratory at the Department of Electrical and Computer Engineering of Florida International University, Miami, FL USA as a postdoctoral researcher. Her research interests are in the area of electromagnetic field numerical calculation and modeling of electric machines. She has 7 journal and 30 conference publications. She became a senior IEEE member in 2004.

Dr. Zhiqiang LIU. Dr. Liu received his Ph.D. from Tianjin University, China in 2002. He was an associate professor at the Department of Industrial Engineering and Automation at Hebei University of Technology, Tianjin, China. Currently he is working in the Energy Systems Laboratory at Florida International University, Miami, FL USA as a visiting researcher. His research interests are in the areas of power electronics and motor drive.